Fuel

A new WSGG radiation model of CO/CO2 mixed gas for solar-driven coal/biomass fuel gasification

--Manuscript Draft--

Manuscript Number:	JFUE-D-23-00229
Article Type:	Research Paper
Keywords:	solar; gasification; radiation; CO; WSGG model
Corresponding Author:	Shiquan Shan, Ph.D Zhejiang University Hangzhou, CHINA
First Author:	Qi Zhang
Order of Authors:	Qi Zhang
	Shiquan Shan, Ph.D
	Zhijun Zhou
	Kai H. Luo
Abstract:	Gasification driven by solar energy with CO2 is an ideal way of low-carbon resource utilization. However, there is a lack of research on the radiation heat transfer process which is important in gasification simulation. In this study, we developed a new the weighted-sum-of-gray-gases (WSGG) model to calculate the radiation heat transfer properties of CO and CO2 mixtures in solar-driven coal/biomass fuel gasification. Benchmarked against the statistical narrow-band model (SNB) of the EM2C laboratory, the WSGG model is suitable for the temperature range of 400-2500 K and the path length range of 0.001-60 m. This study also explored the effect of the CO/CO2 molar ratio on the overall emissivity of the mixture. Furthermore, the model introduces a pressure term into the emissivity calculation process and broadens the pressure range (1 bar, 5 bar, 45 bar). For the first time, the WSGG model is applied to the case where the H/C element ratio is 0, and the fluctuating temperature distribution case (1000 – 2000 K) is analyzed, which is suitable for coal/biomass fuel gasification. In addition, this study calculated the one-dimensional radiation transfer equation, and the results show that the new WSGG has good consistency with the SNB benchmark model under different conditions and can calculate the radiation heat transfer process accurately. Meanwhile, this study also clarified the effect of pressure on the radiation heat transfer with different temperatures.
Suggested Reviewers:	Chungen Yin, Dr. Professor, Aalborg University chy@et.aau.dk Professor Yin is an expert in fuel combustion and numerical calculation
	Yu Lv, Dr. Professor, Mississippi State University ylv@ae.msstate.edu Dr Lv is an expert in energy system research and combustion technology
	Xiuxia Zhang, Dr. Professor, China University of Petroleum Huadong - Qingdao Campus zhangxx@upc.edu.cn Prof Zhang is an expert in gasification simulation
	Kaidi Wan, Dr. Professor, Beihang University wankaidi@buaa.edu.cn Professor Wan is an expert in combustion and fossil fuel energy conversion
	Qiang Yao, Dr. Professor, Tsinghua University yaoq@tsinghua.edu.cn Professor Yao is a senior expert in combustion science

Powered by Editorial Manager® and ProduXion Manager® from Aries Systems Corporation

Dear Professor,

We want to submit our manuscript entitled "*A new WSGG radiation model of CO/CO_2 mixed gas for solar-driven coal/biomass fuel gasification*" for publication in *FUEL*.

In recent years, many countries have announced carbon-neutral energy policies. Low-carbon utilization of carbonaceous feedstocks (coal, biomass, etc.) will play an essential role in this strategy. The gases act as a radiation medium and transfer the energy supplied by the solar energy to the carbon-containing feedstocks for gasification reaction. The current WSGG radiative model mainly considers H_2O and CO_2 as the radiation medium, while the radiation medium in the solar gasification process is CO and CO_2. Therefore, new WSGG radiative models need to be developed for solar gasification.

This study independently developed a new WSGG model under solar gasification and the WSGG model is applied to the case where the H/C element ratio is 0 for the first time. According to the application background of gasification engineering, the applicable pressure range of the model (1 bar, 5 bar, and 45 bar) was expanded, and the fluctuating temperature conditions (1000 – 2000 K) were analyzed. Based on the DOM, this study solved 1-D RTE for three typical conditions (isothermal homogeneity, non-isothermal homogeneity, and non-isothermal non-homogeneity) under three different typical pressures (1 bar, 5 bar, 45 bar). The results show that the difference in the average radiation source term between the new WSGG model and the benchmark SNB model is within 5% in common solar gasification engineering conditions (5 bar, 5 m). The above results show that the new WSGG model will provide an accurate model for applying solar gasification engineering.

The manuscript is checked in **CrossCheck** and revised based on the check results. Moreover, a native speaker with expertise in gasification edits the manuscript to polish it. The work described is original research that has not been published previously and is not under consideration for publication elsewhere, in whole or in part. We greatly appreciate your time to review our manuscript, and we are looking forward to hearing from you soon.

Yours, Sincerely
Shiquan Shan

Highlights

1 A new WSGG radiative model is developed for gases medium in solar gasification.

2. The model is verified and detailed parameters are provided for CFD calculation.

3 The model is applicable for mixtures where the fuel H/C ratio is 0.

4 Pressure is considered in the absorption, broadening the model's applicability range.

5 Effects of *P*, *T*, and *L* on the radiation heat transfer of gas mixtures are revealed.

Manuscript Click here to access/download;Manuscript;manuscript.docx

A new WSGG radiation model of CO/CO_2 mixed gas for solar-driven coal/biomass fuel gasification

Qi Zhang[a,b], Shiquan Shan [a, *], Zhijun Zhou [a], Kai H. Luo [b]

[a] State Key Laboratory of Clean Energy Utilization, Zhejiang University, Hangzhou 310027, Zhejiang, P.R. China; [b.] Department of Mechanical Engineering, University College London, Torrington Place, London WC1E 7JE, UK

*Corresponding author e-mail: shiquan1204@zju.edu.cn

Abstract

Gasification driven by solar energy with CO_2 is an ideal way of low-carbon resource utilization. However, there is a lack of research on the radiation heat transfer process which is important in gasification simulation. In this study, we developed a new the weighted-sum-of-gray-gases (WSGG) model to calculate the radiation heat transfer properties of CO and CO_2 mixtures in solar-driven coal/biomass fuel gasification. Benchmarked against the statistical narrow-band model (SNB) of the EM2C laboratory, the WSGG model is suitable for the temperature range of 400-2500 K and the path length range of 0.001-60 m. This study also explored the effect of the CO/CO_2 molar ratio on the overall emissivity of the mixture. Furthermore, the model introduces a pressure term into the emissivity calculation process and broadens the pressure range (1 bar, 5 bar, 45 bar). For the first time, the WSGG model is applied to the case where the H/C element ratio is 0, and the fluctuating temperature distribution case (1000 – 2000 K) is analyzed, which is suitable for coal/biomass fuel gasification. In addition, this study calculated the one-dimensional radiation transfer equation and the results show that the new WSGG has good consistency with the SNB benchmark model under different conditions and can calculate the radiation heat transfer process accurately. Meanwhile, this study also clarified the effect of pressure on the radiation heat transfer with different temperatures.

Key words: solar; gasification; radiation; CO; WSGG model

---

1 Introduction

In the global context of low-carbon energy strategies, more and more countries are implementing new energy policies to gradually replace traditional fossil energy utilization methods, including the EU's 2050 plan [1] and China's 3060 plan [2]. Low-carbon utilization of carbonaceous feedstocks (coal, biomass, etc.) will play an essential role in this strategy. Furthermore, solar energy is a sustainable energy source that has received extensive attention. Concentrated solar energy can generate higher temperatures [3], which is especially suitable for gasifying carbonaceous feedstocks. Combining solar energy and gasification will be an effective way to realize this energy strategy.

Gasification is an endothermic process powered by the combustion of feedstocks [4]. Figure 1 shows the idea of combining solar energy and gasification. Furthermore, CO_2 collected in the carbon capture and storage (CCS) process is used as a gasification agent to gasify the carbon-containing feedstocks. The energy required for gasification is collected from solar by the concentrating system. In the reactor, the carbon-containing feedstock first undergoes pyrolysis. Then CO_2 and a small amount of H_2O produced by the pyrolysis as gasification agents reduce the char to CO and a small amount of H_2. This process can be regarded as solar energy being fixed as chemical energy, which is also a solar energy storage process, and the entire reaction process is also a Carbon Capture, Utilization, and Storage (CCUS) process [5].

After the solar gasification process reaches a steady state, CO and CO_2 will fill the reactor. During solar gasification, coal is pyrolyzed to produce an amount of H_2O and

CO_2. H_2O participates in the gasification process (mainly consumed by the water-gas shift reaction [6]). Therefore, there is no H_2O in the flue gas. The amount of CO_2 used as a gasification agent is relatively large, and CO_2 still occupies a particular share in the flue gas. As a gasification product, CO is the most abundant in the stabilized reactor atmosphere. As a gas radiation medium, diatomic symmetric molecules such as H_2 and O_2 are transparent media. Triatomic molecules such as CO_2 and H_2O have strong radiation transfer capabilities; also, asymmetric molecules such as CO have specific radiation capabilities [7]. Therefore, from the point of view of both component content and medium radiation capacity, the radiation medium for solar gasification of the type designed in this paper mainly contains two gases: CO and CO_2. The gases act as a radiation medium and transfer the energy supplied by the solar energy to the carbon-containing feedstocks for gasification reaction. To better study the gas radiation transfer process and solve the medium heat transfer problem encountered in the actual solar gasification, we investigated the WSGG model based on CO/CO_2 medium to accurately calculate the radiation transfer process.

As early as the 1970s, Smith et al. [8] developed the WSGG model coefficients suitable for fuel combustion, widely used in numerical simulations. However, this model only applies to the combustion process with air as the oxidant. Considering that the atmosphere of solar gasification contains a lot of gases such as CO, its radiation characteristics are very different from those of combustion. Meanwhile, in recent years, researchers have developed WSGG models based on different benchmark methods. Yin

[9] and Rehfeldt [10] used the EWBK model as a benchmark for development; Johansson et al. [11] used the SNB model of the EM2C database developed as a benchmark; Tanin [12] and Leonardo [13] gave their respective models using the more accurate HITEMP2010 database. In the above, Yin, Johansson, Tanin, and others provided detailed model coefficients, while only Tanin and Leonardo gave the coefficient determination method. Many researchers have recently developed different WSGG models for different application backgrounds. Alexandre et al. [14] developed a fitting procedure for WSGG. They introduced a new formula for the appropriate approach at constant pressure to account for the molar ratio of H_2O and CO_2, reducing the dependence on interpolation. Xuan et al. [15] applied the WSGG model of H_2O/CO_2 to aero engines combustion and broadened its pressure range to 30 atm. Wu et al. [16] added CO as a radiation medium to the WSGG model and analyzed the gas radiation model's effect on the wall's radiation heat flux.

Shan et al. [17] developed a WSGG model for oxy-fuel combustion and coupled pressure factors into the model. Meanwhile, Shan et al. [18] also analyzed the effect of pressure on the radiative heat transfer of the H_2O/CO_2 mixture. Cai et al. [19] developed an $H_2O/CO_2/CO$ radiation transfer model for pulverized coal Gaskombiant Schwarze Pumpe (GSP) gasifier under typical pressure (45 atm) and compared and analyzed the effect of CO on gas radiation heat transfer under the background of pulverized coal gasification at a specific pressure.

The H / C element molar ratio in the existing WSGG model is 8-0.25. The ratio of solar gasification with CO_2 as the gasification agent is 0. The current WSGG model uses H_2O and CO_2 as the radiation medium, while the radiation medium in the solar gasification process is CO and CO_2. Therefore, new WSGG models need to be developed for solar gasification.

Gasification is a complex reaction [20]. Generally, gasification can be promoted by increasing the temperature, pressure, or catalyst [6, 21]. Furthermore, the standard approach for solar gasification engineering applications and an economical point of view is to increase the pressure. Joint pressures for existing gasifiers in production are 1 bar, 5 bar, and 45 bar. However, the existing WSGG model coefficients are all for oxy-fuel combustion under atmospheric pressure. Recent studies [17] reported that the results obtained by extrapolating the WSGG model for atmospheric combustion to high-pressure conditions are not ideal. There is no report on the WSGG model coefficients for the pressurized solar gasification gas radiation characteristics. Therefore, developing a model for the radiation characteristics of pressurized gas under solar gasification flue gas (CO and CO_2) is urgent.

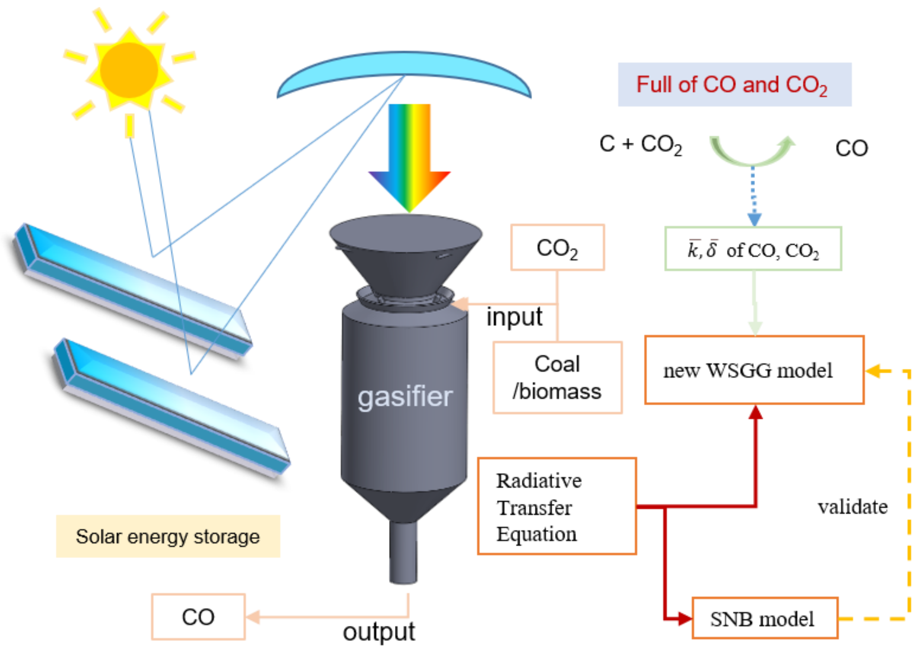

Figure 1 Development route of solar gasification gas radiation model

To sum up, the route of solar gasification is in line with the carbon-neutral energy demand of countries worldwide and has significant strategic value. Radiation transfer in the gaseous medium is a fundamental scientific problem in this route. We independently developed a new WSGG model under solar gasification and analyzed the effect of pressure on the radiation heat transfer of CO/CO_2 mixed gas. The innovations of this study are as follows: (1) In this investigation, a new WSGG model is developed according to the characteristics of solar gasification flue gas components (CO and CO_2); the WSGG model is applied to the case where the H/C element ratio is 0 for the first time. (2) According to the application background of gasification engineering, the applicable pressure range of the model (1 bar, 5 bar, and 45 bar) was expanded, and the fluctuating temperature conditions (1000 – 2000 K) were analyzed. (3) This study is based on the DOM solving a one-dimensional case of the Radiative Transfer Equation (RTE). These results will provide a reference for the engineering application of solar gasification and give a more accurate gas radiation model for the numerical simulation of the process.

2 Methods

2.1 SNB model

There are three main methods for calculating the radiation characteristics of the medium and high temperature (less than 3000 K) gases: line-by-line calculation method [22], narrow-band model [23], and broad-band and other spectral-band models [24]. The narrow-band model is to conform the spectral intensity and position distribution within a specific wavenumber interval to a particular law, expresses it in a mathematical function, and then determines it according to the experimental data so the result is more accurate. Among them, the statistical narrow-band (SNB) model considers that spectral line position and intensity distribution are random. To calculate the radiation characteristics of the carbon dioxide 12 um band, the LBL model needs to figure 18566 spectral lines. In contrast, the narrow-band model method only needs to calculate 16 narrow bands. Besides that, the SNB model dramatically simplifies the calculation process while ensuring accuracy and is suitable for the model development of this investigation.

The SNB model was proposed in 1967 by Malkmus [25]. As mentioned earlier, the SNB model requires fitting to experimental data. Among the many databases of the statistical narrow-band model, the parameters of the SNB model established by the French EM2C laboratory data are the closest to the results of the line-by-line method model developed based on the HITEMP 2010 database [7, 23]. The SNB model based on the EM2C laboratory development is widely used as a benchmark [17-19, 26-28].

In this model, the expression for the average transmittance is：

$$\bar{\tau} = \exp\left[-\frac{2\bar{\gamma}}{\bar{\delta}}\left(\sqrt{1+\frac{XPL\bar{k}\bar{\delta}}{\bar{\gamma}}}-1\right)\right] \tag{1}$$

where $\bar{\gamma}$ is Lorentzian half-widths, $\bar{k}$ and $\bar{\delta}$ are provided by EM2C laboratory.

The Lorentzian half-widths of the mean lines of CO and CO_2 are expressed as：

$$\bar{\gamma}_{CO_2} = \frac{p}{p_s}\left(\frac{T_s}{T}\right)^{0.7}\left[0.07x_{CO_2} + 0.058\left(1 - x_{CO_2}\right)\right] \tag{2}$$

$$\bar{\gamma}_{CO} = \frac{p}{p_s}\left\{0.075x_{CO_2}\left(\frac{T_s}{T}\right)^{0.6} + 0.06\left(1 - x_{CO_2}\right)\left(\frac{T_s}{T}\right)^{0.7}\right\} \tag{3}$$

where $p_s = 1\,bar$, $T_s = 296\,K$.

Table 1 Min and max SNB model band centers and the total number of bands.

molecular	v_{min} (cm^{-1})	v_{max} (cm^{-1})	Bands
CO	1600	6425	194
CO_2	250	8300	323

2.2 WSGG model

Hottel [29] proposed the weighted-sum-of-gray-gases（WSGG）model and applied it to calculate the radiative transfer process. Besides, the model's gas components are H_2O and CO_2 at this stage. At the same time, the pressure change is not coupled to the model. The WSGG model focuses on replacing multiple non-gray gases with n gray gases. The absorption coefficient or radiant heat flux is represented by the weighted sum of the calculated values of the n gray gases [17].

For the WSGG model, the expression for emissivity over path-length (L) thread length is:

$$\varepsilon = \sum_{i=1}^{n} a_i\left[1 - exp(-\kappa_i xPL)\right] \tag{4}$$

where x is the sum of the mole fractions of CO and CO_2 in the mixed gas:

$$x = x_{CO} + x_{CO_2} \tag{5}$$

Although Eq. (5) contains the pressure term, the coefficient under normal pressure still cannot meet the requirements of high-pressure calculation [17]. Therefore, this investigation will develop the coefficients suitable for high-pressure conditions and combine the pressure parameter P with the absorption coefficient k to obtain a new WSGG model emissivity expression:

$$\varepsilon = \sum_{i=1}^{n} a_i \left[1 - exp\left(-\kappa_{i(45bar)} xL\right)\right] \tag{6}$$

Different absorption coefficients κ_i were developed for the gasification industry's typical pressures of 1 bar, 5 bar, and 45 bar. At the same time, Robert et al. [11] believed that the model's accuracy was higher when fitting the calculation with four kinds of gray gases, n = 4. In addition, the weight value a_i is a temperature-related coefficient, and its expression is:

$$a_i = \sum_{j=0}^{m} c_{i,j} \left(\frac{T}{T_{ref}}\right)^m \tag{7}$$

where Yin et al. [9] believed that introducing the reference temperature, T_{ref}, could make the coefficient $c_{i,j}$ dimensionless and improve the model's accuracy. Reference [15] recommended reference temperature $T_{ref} = 2000$ K.

Tain and Robert et al. [23] obtained the relationship between the coefficients $c_{i,j}$ and κ_i and different molar ratios of H_2O and CO_2 through the polynomial fitting. Inspired by this, this investigation gets the relationship between coefficients $c_{i,j}$ and κ_i and different molar ratios of CO_2 and CO using the polynomial fitting:

$$c_{ij} = A1_{ij} M^2 + B1_{i,j} M + C1_{i,j} \tag{8}$$

$$\kappa_i = A2_i M^2 + B2_i M + C2_i \tag{9}$$

where the database of this model is attached in Appendix A. M represents the molar ratio of CO_2 to CO:

$$M = x_{CO_2}/x_{CO} \tag{10}$$

2.3 Radiative Transfer Equation (RTE)

2.3.1 Equation Solving

For an emitting-absorbing and non-scattering medium, the RTE can be written as [12] :

$$\frac{\partial I_\eta(r,\hat{S})}{\partial S} = \kappa_\eta I_{b,\eta}(r) - \kappa_\eta I_\eta(r,\hat{S}) \tag{11}$$

where I_η represents the spectral emission intensity, $I_{b,\eta}$ is the blackbody spectral emission intensity.

The radiative transfer calculation for the whole space is to calculate the RTE for the entire spectrum and all spatial directions. Applying the Discrete-Ordinates Method (DOM) to the RTE for any of the four grey gases, the RTE can be written in the following form [15]:

$$\frac{dI_i(r,\hat{S})}{dS} = \kappa_i a_i I_{b,\eta}(r) - \kappa_i I_i(r,\hat{S}) \tag{12}$$

where $I_{b,\eta}(r) = \sigma T^4(r)/\pi$。 Figure 2 shows the process of solving RTE by the DOM. The one-dimensional radiation transfer is divided into positive and negative directions. The cosine of the angle between each direction and the r-axis is μ_i, and the weight is w_i. Meanwhile, the boundary condition is a black body wall, so the RTE in each direction can be expressed as:

$$\mu_i \frac{dI_i^+(r,\hat{S})}{dr} = \kappa_i a_i(r) I_{b,\eta}(r) - \kappa_i I_i^+(r,\hat{S}) \tag{13}$$

$$-\mu_i \frac{dI_i^-(r,\hat{S})}{dr} = \kappa_i a_i(r) I_{b,\eta}(r) - \kappa_i I_i^-(r,\hat{S}) \tag{14}$$

$$\tau = 0: I_i^+(r_0) = I_{b,i}(r_0) \quad (15)$$

$$\tau = \tau_l: I_i^-(r_s) = I_{b,i}(r_s) \quad (16)$$

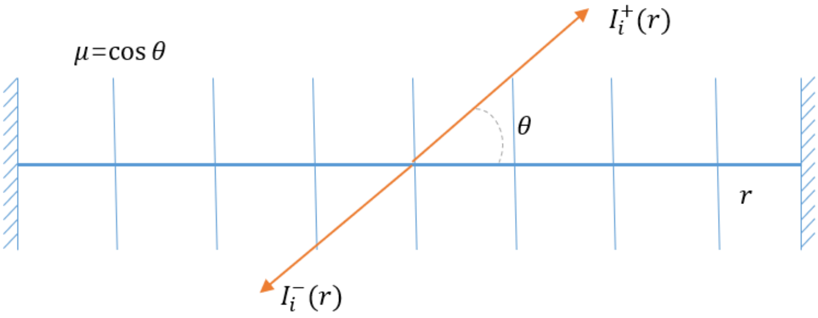

Figure 2 Calculation process of DOM

This medium radiation process is discretized into n computing units. After calculating the radiation intensity by point along the route, the radiation heat flow and radiation source terms of each issue are obtained as follows:

$$\mathrm{q}_t = \sum_i \sum_l 2\pi\mu_l w_l [I_i^+(r_t, l) - I_i^-(r_t, l)] \quad (17)$$

$$\dot{\mathrm{q}}_t = \sum_i \sum_l \{2\pi\kappa_i w_l [I_i^+(r_t, l) + I_i^-(r_t, l)] - 4\pi\kappa_i w_l I_{b,i}(r_t)\} \quad (18)$$

Among them, the radiation source term can be coupled with CFD calculation and applied in the numerical simulation of solar gasification [9, 16, 19].

2.3.2 SNB coupled RTE solution

It can be seen from Section 2.1 that, based on Equation (4) in the solution process of the SNB model, the average emissivity can be solved by the transmittance:

$$\bar{\varepsilon}_L = 1 - exp(-\bar{\kappa}xPL) \quad (19)$$

When the radiation transfer equation in the whole radiation space is solved, within each unit travel length (Δr), CO and CO_2 gases are considered to be isotropic. In this way, the absorption coefficient can be calculated from the transmittance of each Δr:

$$\frac{dI_v(r,\hat{S})}{dS} = \kappa_v a_v I_b(r) - \kappa_v I_v(r,\hat{S}) \quad (20)$$

Similarly to 2.3.1, the radiation transfer equations on each spectral band are solved and summed by the DOM. Then the radiation heat flux and radiation source terms are calculated.

2.4 Coal gasification 1 - D heat transfer case settings

The coal gasification temperature is high, and the biomass gasification temperature is low. We set up three working conditions for the situations often encountered in practice. The three working conditions are isothermal homogeneous, non-isothermal homogeneous, and non-isothermal non-homogeneous in Table 2 – Table 4. Setting the wall temperature of 1000 K, the temperature distribution between the plates is:

$$T = 1500 - 500\,cos(\frac{2\pi s}{L})\ \ (K) \tag{21}$$

$$T = 1500 - 300\,cos(\frac{2\pi s}{L})\ \ (K) \tag{22}$$

$$T = 1500 - 100\,cos(\frac{2\pi s}{L})\ \ (K) \tag{23}$$

Table 1. isothermal and homogeneous case conditions (Case 1 series)

	Non-isothermal homogeneous					
Case	*T* (K)	*P* (bar)	X_{CO2}	X_{CO}	M	*X*
1.1	1000	1, 5, 45				
1.2	1300	1, 5, 45				
1.3	1500	1, 5, 45	0.18	0.72	0.25	0.9
1.4	1700	1, 5, 45				
1.5	2000	1, 5, 45				

Table 2. Non-isothermal and homogeneous case conditions (Case 2 series)

	Non-isothermal homogeneous					
Case	*T* (K)	*P* (bar)	X_{CO2}	X_{CO}	M	*X*
2.1	Eq.(21)					
2.2	Eq.(22)	1, 5, 45	0.18	0.72	0.25	0.9
2.3	Eq.(23)					

Meanwhile, the gas components between the plates are:

$$x_{CO2} = 0.15 + 0.03\cos\left(\frac{2\pi s}{L}\right) \tag{24}$$

$$x_{CO} = 0.6 + 0.12\cos\left(\frac{2\pi s}{L}\right) \tag{25}$$

Table 3. Non-isothermal and non-homogeneous case conditions (Case 3 series)

Non-isothermal non-homogeneous						
Case	*T* (K)	*P* (bar)	X_{CO2}	X_{CO}	M	*X*
3.1	Eq. (21)					
3.2	Eq. (22)	1, 5, 45	Eq. (24)	Eq. (25)	0.25	0.48-0.72
3.3	Eq. (23)					

3 Results and discussion

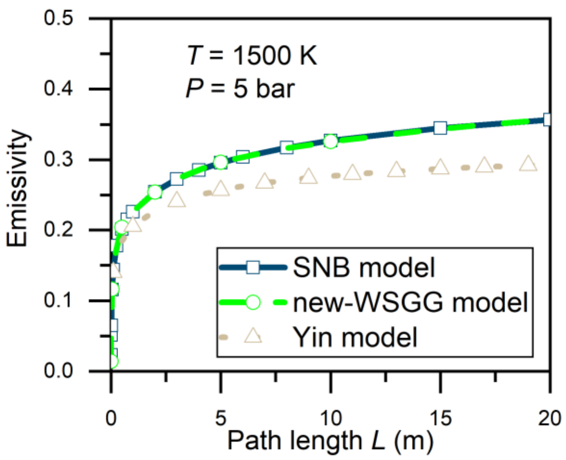

Figure 3 Path length evolution of emissivity

The triangle in Fig. 3 shows the path length evolution of emissivity when calculating a mixture of CO and CO_2 (M = 2) at 1500 K, 5 bar by the classical Yin gas radiation model [9]. Although the coefficients of the Yin model under normal pressure conditions can be calculated by extrapolating the formula to high-pressure situations, there is a certain degree of error, as shown in Figure 3, and the results are inaccurate. Since the Yin model does not consider CO gas, the calculated gas medium emissivity has a more significant error than the benchmark SNB model. However, the new WSGG model considers the CO component, and its estimated emissivity distribution along the path matches the benchmark model well. After verification of this result, the existing WSGG cannot accurately calculate the radiation transfer process of the medium with high CO concentration under the background of solar gasification, so we need to develop a new gas radiation model. The new WSGG model is in excellent agreement with the SNB model and can be used in the simulation calculation of actual engineering.

3.1 Emissivity calculation results

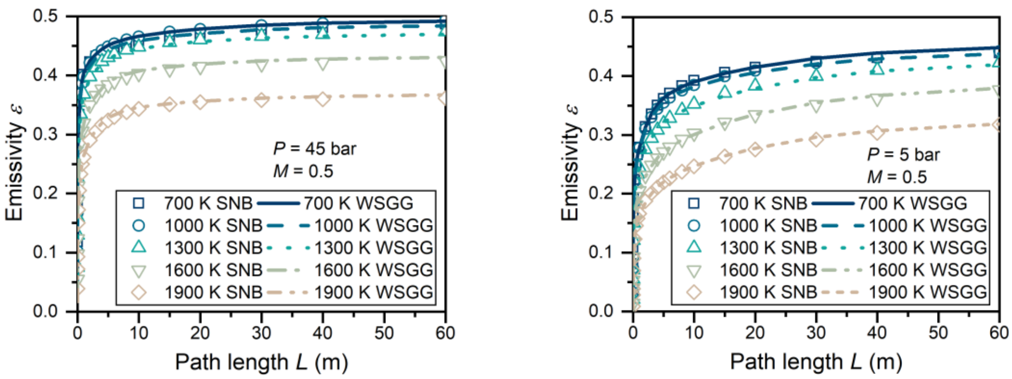

(a) P=45 bar, M = 0.5 (b) P=5 bar, M = 0.5

Figure 4 The path evolution of mixed gas emissivity at different temperatures

The gasification reaction is endothermic and significantly affected by temperature changes [30]. Therefore, exploring the emissivity distribution of the radiation medium (CO and CO_2 mixture) at different temperatures is necessary. Figure 4 shows the emissivity distribution from 0 – 60 m for a mix of CO and CO_2 (P = 5 / 45 bar, M = 0.5) at different temperatures. The emissivity rises with the path length in the 0 – 60 m range. After the path length reaches about 10 m, the emissivity remains unchanged.

In Figure 4, the new WSGG model results are consistent with the benchmark model. In addition, the temperature increases from 700 K, and the emissivity first decreases slowly. Above 1300 K, the temperature increase enhances the drop's magnitude of emissivity, which is consistent with the results in the literature [17, 18].

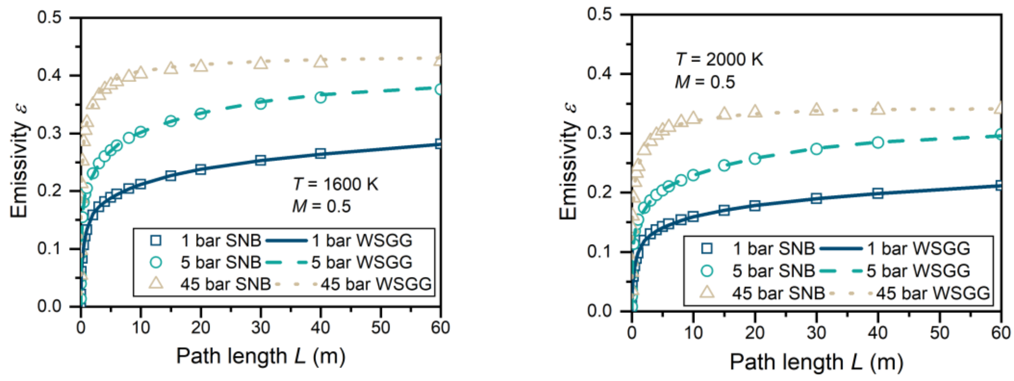

(a) T = 1600 K, M = 0.5　　(b) T = 2500 K, M = 0.5

Figure 5 The path evolution of mixed gas emissivity at different pressures

There are three main types of pressure gasifiers in operation: normal pressure (1 bar), pressurized (5 bar), and high pressure (45 bar). The existing experiments of solar gasification are all carried out under normal pressure[4, 31-33]. To cover the pressure range and to explore the future of solar gasification at pressurized and high pressure, the gas radiation model in this investigation covers 1 bar, 5 bar, and 45 bar. Figure 5 shows the distribution of the mixed gas emissivity along the path at different pressures (T = 1600 K, M = 0.5). In the 0 – 60 m range, the emissivity sees an increase as the path increases. Emissivity remains essentially unchanged after reaching approximately 40 (1 bar), 30 (5 bar), and 20 (45 bar) m. When the pressure increased from 1 bar to 5 bar, the emissivity of the mixed gas medium rose significantly. From 5 bar to 45 bar, the emissivity continued to grow, but the magnitude of the increase decreased.

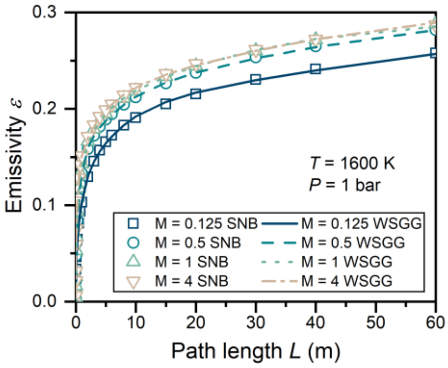

(a) P = 1 bar, T = 1600 K

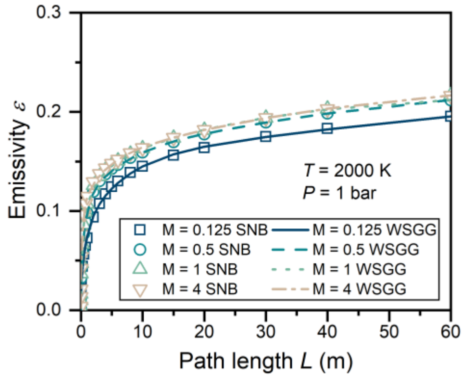

(b) P = 1 bar, T = 2000 K

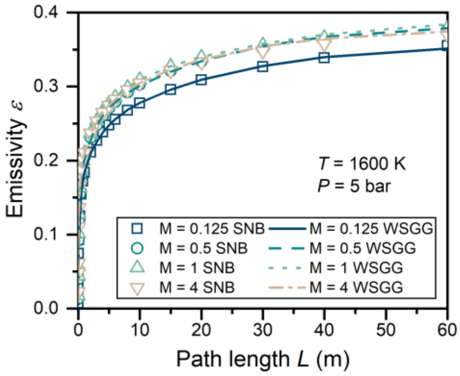

(c) P = 5 bar, T = 1600 K

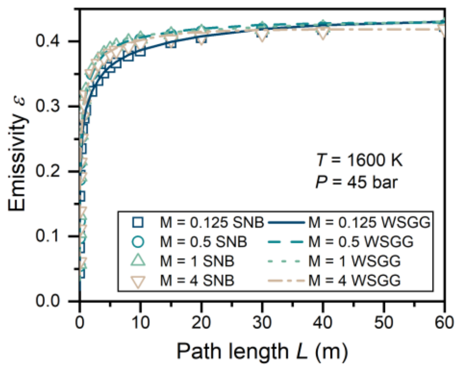

(d) P = 45 bar, T = 1600 K

Fig.6 Path length evolution of mixed gas emissivity with different molar ratios

The proportion of gas in the solar gasification reactor varies from place to place, showing a fluctuating trend. Figure 6 shows the distribution of the mixed gas emissivity along the path at different molar ratios and pressures. The emissivity results calculated by the new WSGG model are in good agreement with those of the benchmark model under normal, pressurized, or high-pressure conditions. Comparing Figure 6 (a) and Figure 6 (b) at the same pressure (1 bar), an increase in temperature leads to a decrease in emissivity. Comparing Figure 6 (a), (c), and (d), under the same molar ratio, the emissivity of the mixed gas increases with pressure. Meanwhile, with the rise of the molar ratio, the emissivity increases; this is because the proportion of CO_2 in the flue gas increases, and the radiation ability of triatomic polar molecules is more substantial than that of binary molecules CO.

3.2 Isothermal homogeneous cases of radiation transfer characteristics

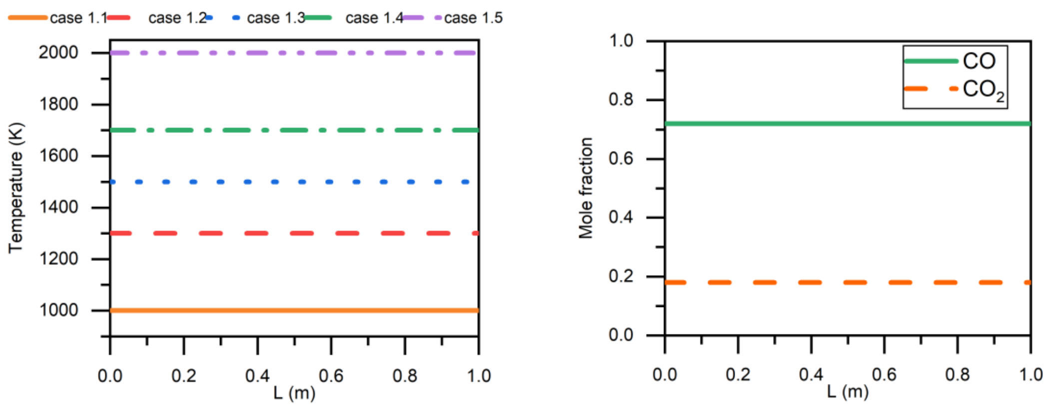

(a) Temperature (b) Gas components

Figure 7 Distribution of isothermal homogeneous cases between plates

Figure 7 shows the temperature and gas components distribution under homogeneous isothermal conditions. Besides, the distribution of the components is an example of typical distribution in solar gasification. Figure 7 (a) covers the temperature range from 1000 – 2000 K, and Figure 7 (b) shows the homogeneous distribution of CO and CO_2 mole fractions.

To evaluate the new WSGG model, we investigated the gas region's radiation heat flux and radiation source terms between two infinite black parallel plates. Test cases cover various temperature conditions to illustrate the model's ability to handle multiple computational problems in gasification applications. The reactor outlet of the solar gasification reaches the stable flue gas temperature, and the flue gas composition is stable.

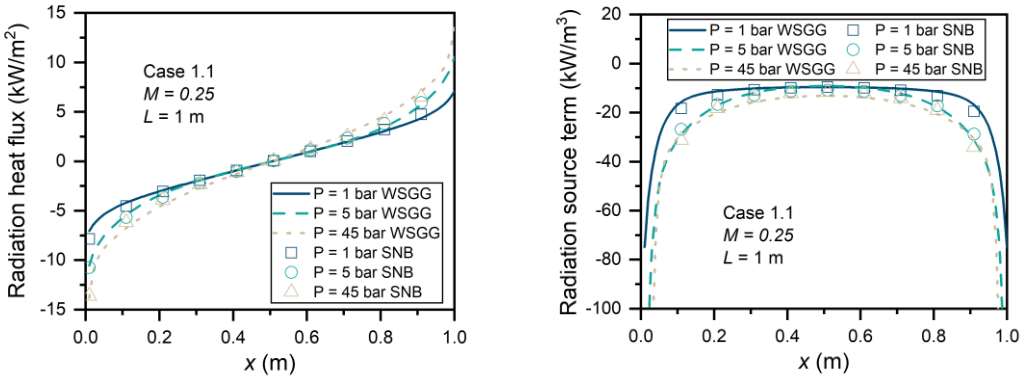

(a) Evolution of radiation heat flux at different pressure

(b) Evolution of radiation source term at different pressure

Figure 8 Effect of pressure on radiation heat flux and radiation source term between plates

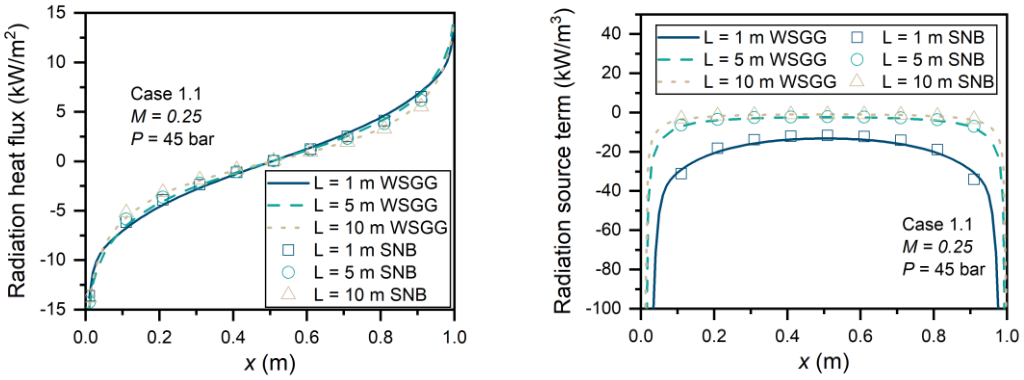

(a) Evolution of radiation heat flux at different path lengths

(b) Evolution of radiation source term at different path lengths

Figure 9 Effect of path length on radiation heat flux and radiation source term between plates

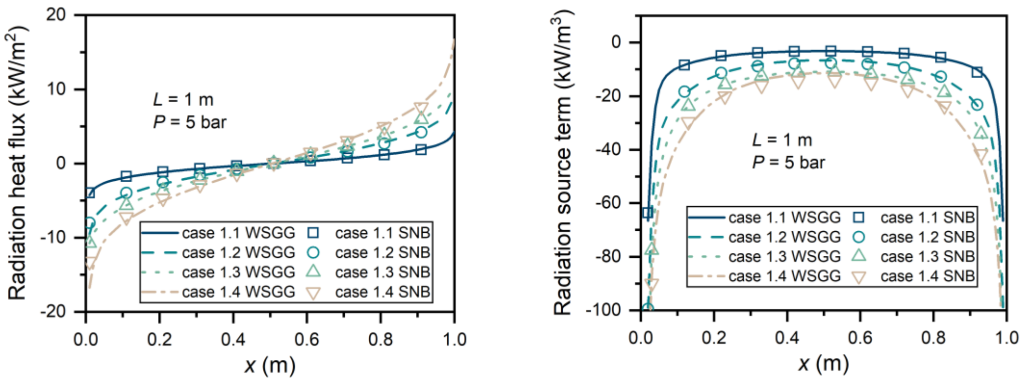

(a) Evolution of radiation heat flux

(b) Evolution of radiation source

at different temperatures | term at different temperatures

Figure 10 Effect of temperatures on radiation heat flux and radiation source term between plates

Figure 8 shows the radiation heat flux and source terms at different pressure (1, 5, 45 bar). Pressure is a common engineering means to improve the conversion rate of solar gasification. The results of the radiation heat flux and radiation source terms calculated by the new WSGG model are in good agreement with those of the benchmark model, whether under normal pressure, pressurized, or high pressure. The trend of radiation heat flux curves under different pressures is similar. But the radiation heat flux increases with pressure, so as the radiation source term. Figure 9 shows that the results are consistent with the benchmark results under different path lengths, such as 1 m, 5 m, and 10 m. Under a 10 m path length, the error of wall heat flux will be higher than 1 m. In general, the longer the path length is, the larger the error of wall heat flux is. Figure 10 shows the effect of different temperatures on the radiation heat flux and radiation source terms for the same path length and pressure. To varying temperatures from case 1.1 to case 1.5, the new WSGG model calculates radiation heat flux and radiant source terms with an error of less than 10 % compared with the benchmark model. Meanwhile, the radiative heat flow increases with temperature, as does the radiation source term.

3.3 Non-Isothermal homogeneous cases of radiation transfer characteristics

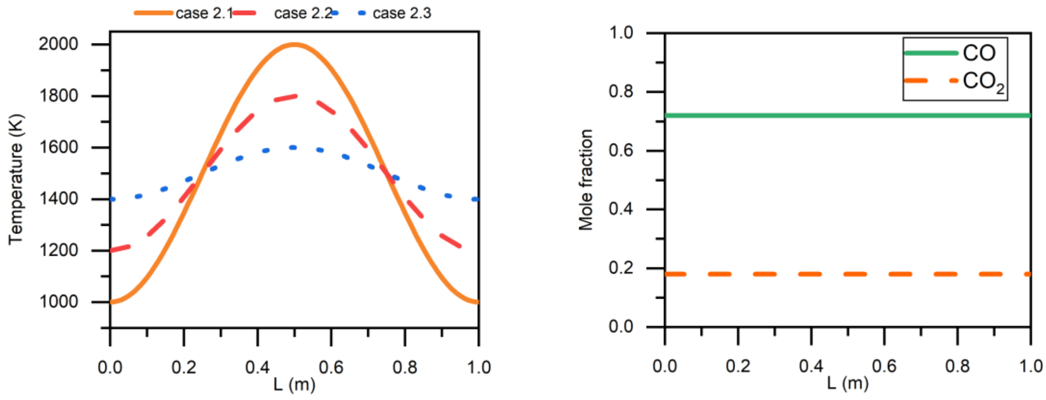

(a) Temperature (b) Gas components

Figure 11 Distribution of isothermal homogeneous cases between plates

Figure 11 shows the gaseous radiation medium's temperature and components distribution under non-isothermal homogeneous conditions. Figure 11 (a) covers the temperature range commonly found in gasification reactors, and Figure 11 (b) shows the CO and CO_2 mole fraction ratios for a uniform distribution. This distribution is because the temperature varies from the gasification reaction zone to the outlet. Therefore, we explored non-isothermal homogeneous working conditions.

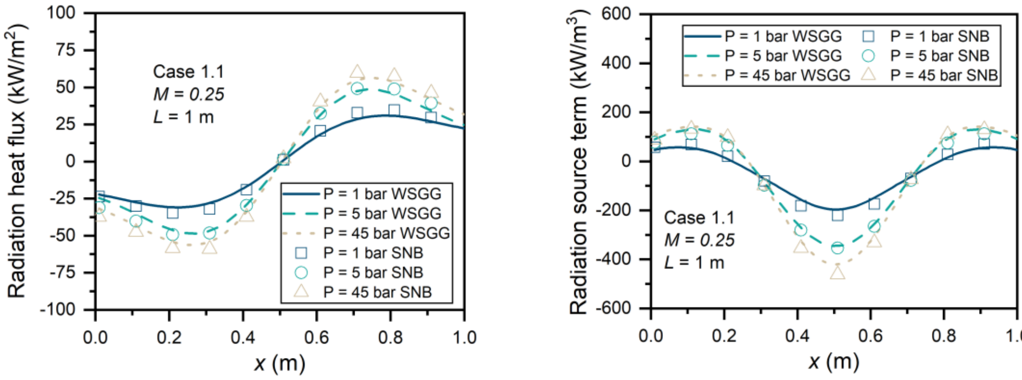

(a) Evolution of radiation heat flux at different pressure

(b) Evolution of radiation source term at different pressure

Figure 12 Effect of pressure on radiation heat flux and radiation source term between plates

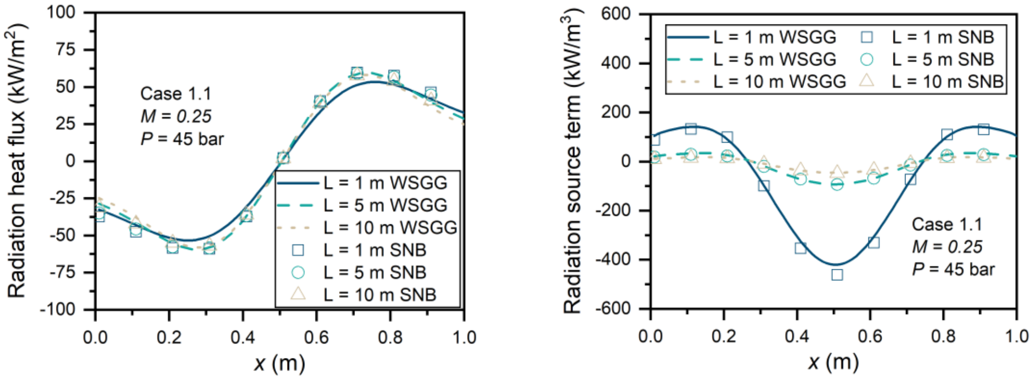

(a) Evolution of radiation heat flux at different path lengths

(b) Evolution of radiation source term at different path lengths

Figure 13 Effect of path length on radiation heat flux and radiation source term between plates

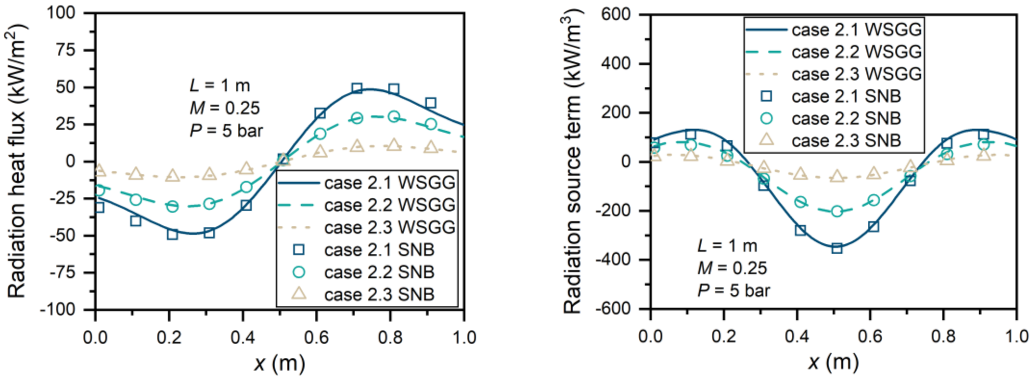

(a) Evolution of radiation heat flux at different wave temperatures

(b) Evolution of radiation source term at different wave temperatures

Figure 14 Effect of waving temperatures amplitude on radiation heat flux and radiation source term between plates

Figure 12 shows the effect of pressure on the radiation heat flux and radiation source terms for the non-isothermally homogeneous case. The average calculation error of the new WSGG model and the benchmark model is within 10%. Besides, it can be provided for the effect of pressure on the gasification reaction: the increase of pressure enhances the radiation heat transfer process. But the continued increase will slow the growth in heat transfer. Figure 13 shows the effect of path variation (1, 5, 10 m) on the radiation heat flux and source terms under non-isothermal homogeneous conditions. At a high pressure of 45 bar, the radiation heat flux does not change much with different path lengths. However, the radiation source term still has a significant effect at high pressures of 45 bar with varying path lengths. Especially at L = 1 m, the radiation source terms are higher than the other paths. Radiation greatly influences the heat transfer process in the short path, and we cannot ignore the effect of gas radiation in the gasification simulation process. Figures 14 (a) and (b) show the effects of different temperature fluctuations on the radiative heat flow and radiation source terms under non-isothermal homogeneous conditions. The error between the new WSGG calculation results and the benchmark model results is within 10%. In the background of solar gasification, temperature fluctuations often occur, so the accurate calculation of radiation heat flux and radiation source terms with different gas components is essential.

3.4 Non - Isothermal non - homogeneous cases of radiation transfer characteristics

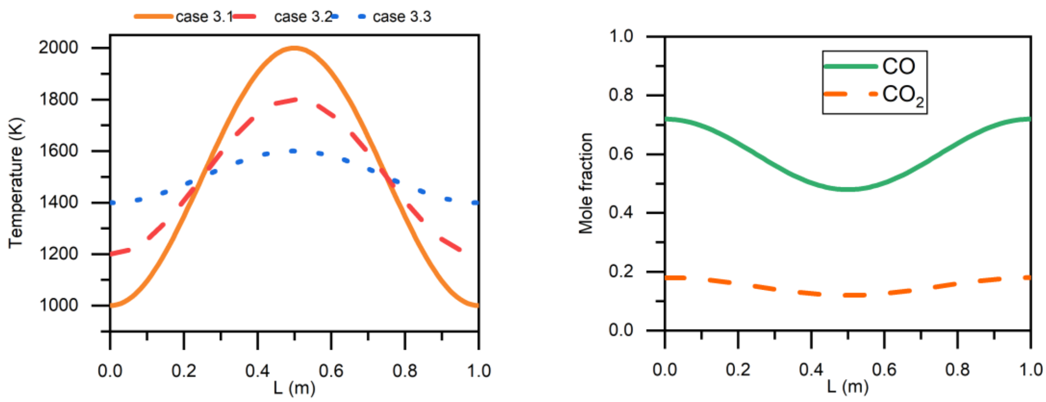

(a) Temperature (b) Gas components

Figure 15 Distribution of isothermal homogeneous cases between plates

Figure 15 shows the gaseous radiation medium's temperature and composition distribution under non-isothermal non-homogeneous conditions. Figure 15 (a) covers the range of temperature variations commonly found in gasification reactors, and Figure 15 (b) shows the CO and CO_2 mole fraction ratios for a non-uniform distribution. It is one of the primary conditions of the gasification reaction zone of solar gasification. Therefore, we explored non-isothermal non-homogeneous working conditions.

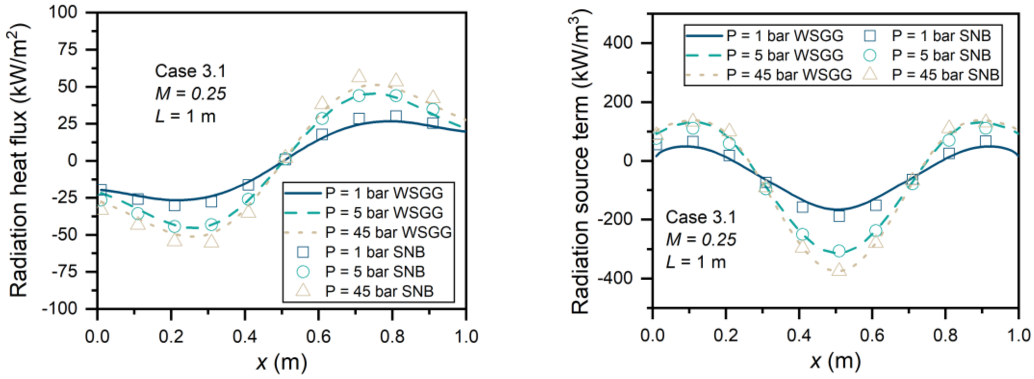

(a) Evolution of radiation heat flux at different pressure

(b) Evolution of radiation source term at different pressure

Figure 16 Effect of pressure on radiation heat flux and radiation source term between plates

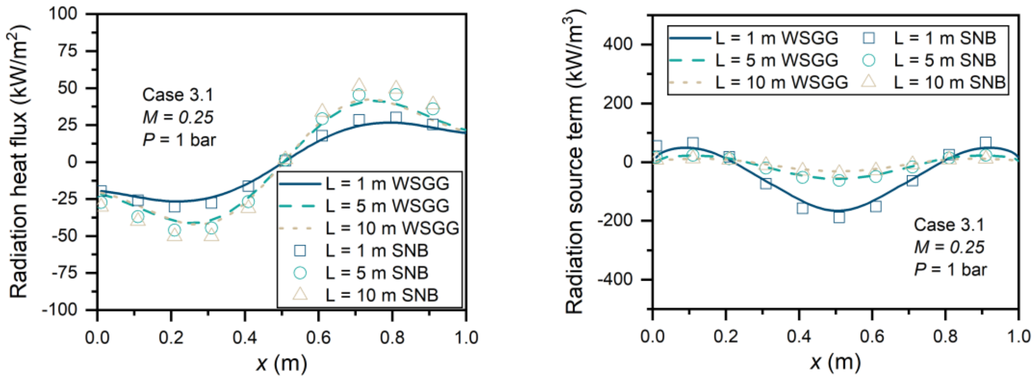

(a) Evolution of radiation heat flux at different path lengths

(b) Evolution of radiation source term at different path lengths

Figure 17 Effect of path length on radiation heat flux and radiation source term between plates

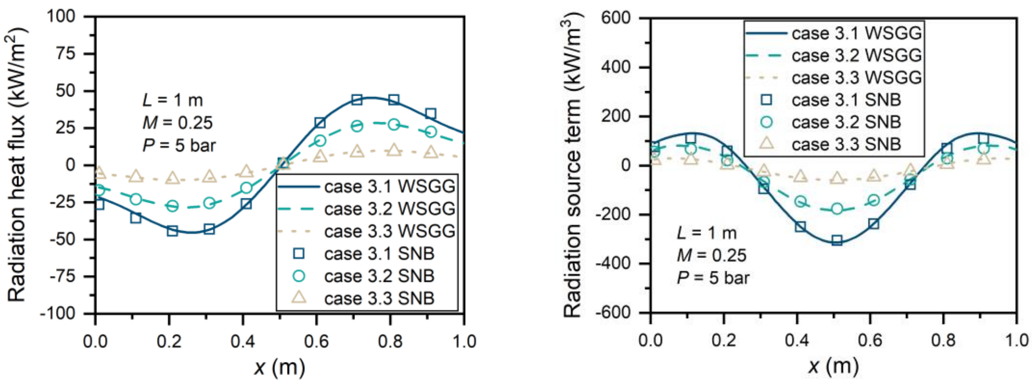

(a) Evolution of radiation heat flux at different wave temperatures

(b) Evolution of radiation source term at different wave temperatures

Figure 18 Effect of waving temperatures amplitude on radiation heat flux and radiation source term between plates

Figures 16 and 17 show the effects of pressure and path lengths on the radiation heat flux and radiation source terms for non-isothermal non-homogeneous conditions. The results calculated by the new WSGG model are within an 8 % error of the benchmark model results. Waving temperature and gas components distribution are closer to the actual situation of engineering applications. As the path decreases, the pressure increases, and the same as the radiation source term does. Figure 18 shows the effects of different temperature amplitude changes on the radiation heat flow and radiation source term. The results of the new WSGG model are within an 8% error of the benchmark model results. Besides, the amplitude change of temperature will lead to a significant difference in the radiation source term—the radiation source term increase with the temperature fluctuation.

3.5 Comparison of various cases

3.5.1 Error analysis

In this paper, we calculated cases of radiative heat transfer between infinite plates under three pressures of 1, 5, and 45 bar, in which the plate spacing is 1 m. Besides, we divided cases into different conditions under the background of solar gasification. All the examples use the SNB model as the benchmark model to analyze the influence of conditions on the radiation heat transfer.

The error between the new WSGG model and the benchmark model is expressed as [18, 19]:

$$\delta q = \frac{|q_{WSGG} - q_{SNB}|}{max|q_{SNB}|} \times 100\% \tag{26}$$

$$\delta \dot{q} = \frac{|\dot{q}_{WSGG} - \dot{q}_{SNB}|}{max|\dot{q}_{SNB}|} \times 100\% \tag{27}$$

where *max* represents the maximum absolute value of the radiation heat flux and the radiation source term in each case. Besides, errors in wall heat flux (δq_{wall}) and midpoint radiation source terms ($\delta \dot{q}_{mid}$) are considered in this investigation. In actual calculations, people often think of the average error. The average error of the radiation heat flux and radiation source terms is defined as:

$$\delta q_{avg} = \frac{\int_0^L |q_{WSGG} - q_{SNB}|}{\int_0^L |q_{SNB}|} \times 100\% \tag{28}$$

$$\delta \dot{q}_{avg} = \frac{\int_0^L |\dot{q}_{WSGG} - \dot{q}_{SNB}|}{\int_0^L |\dot{q}_{SNB}|} \times 100\% \tag{29}$$

Table 5 Errors between the new WSGG model and the benchmark model

Pressure	1 bar				5 bar				45 bar			
Items	δq_{wall}	δq_{avg}	$\delta \dot{q}_{mid}$	$\delta \dot{q}_{avg}$	δq_{wall}	δq_{avg}	$\delta \dot{q}_{mid}$	$\delta \dot{q}_{avg}$	δq_{wall}	δq_{avg}	$\delta \dot{q}_{mid}$	$\delta \dot{q}_{avg}$
L = 1 m												
Case 1.1	8.84	3.72	1.08	1.48	2.31	0.49	0.66	0.45	9.64	0.95	0.01	0.50
Case 1.2	12.12	9.65	2.56	4.36	2.28	1.69	0.45	0.60	2.79	1.64	0.13	0.57
Case 1.3	8.45	2.23	0.07	2.11	2.03	2.07	0.69	1.04	1.53	2.39	0.26	0.82
Case 1.4	10.05	9.12	6.71	9.68	2.49	3.08	0.96	1.32	0.97	2.17	0.27	0.96
Case 1.5	11.47	9.94	6.45	5.96	10.37	6.54	1.66	1.27	10.29	2.87	0.25	1.16
Case 2.1	1.75	6.91	0.44	7.90	12.32	5.52	2.20	3.69	9.12	6.53	8.92	3.30
Case 2.2	4.81	5.24	1.00	9.67	8.94	3.01	0.40	2.95	2.01	2.84	6.13	2.31
Case 2.3	10.13	1.06	1.95	1.30	5.74	2.07	2.73	3.19	4.32	1.57	2.26	2.16
Case 3.1	2.29	8.07	1.90	9.20	10.14	3.23	2.33	3.80	9.82	8.42	3.35	4.65

Case 3.2	4.50	6.51	3.48	1.55	6.78	2.70	3.85	3.96	2.73	4.87	0.66	3.98
Case 3.3	4.49	0.33	5.69	4.91	3.74	2.97	5.62	4.59	3.57	2.60	6.70	3.91
L = 5 m												
Case 1.1	7.33	3.02	0.18	1.31	5.32	0.48	0.03	0.26	0.82	1.25	0.05	0.15
Case 1.2	11.51	6.45	0.59	2.91	5.47	1.70	0.06	0.31	0.86	1.21	0.03	0.30
Case 1.3	12.41	5.19	1.05	1.55	4.47	1.82	0.06	0.50	3.03	2.57	0.09	0.46
Case 1.4	9.45	7.74	2.73	6.86	5.89	2.34	0.12	0.68	0.66	1.76	0.05	0.46
Case 1.5	11.67	5.21	4.49	10.75	15.24	5.54	0.53	1.18	10.80	5.18	0.33	0.72
Case 2.1	14.61	2.20	2.46	5.70	15.17	3.46	8.31	4.66	11.18	3.02	0.03	3.43
Case 2.2	6.96	8.40	0.50	7.03	10.16	0.44	4.48	4.91	3.27	3.21	5.48	4.11
Case 2.3	9.51	7.87	1.67	8.42	5.60	7.54	1.05	5.03	3.97	6.51	8.96	4.57
Case 3.1	12.51	0.18	9.90	5.17	15.67	3.86	7.58	4.93	11.75	3.05	0.94	3.21
Case 3.2	4.93	6.73	8.83	6.83	10.66	0.85	3.61	5.21	3.17	2.76	3.53	3.57
Case 3.3	1.78	8.58	1.44	0.48	6.19	7.98	0.19	5.34	4.50	6.36	7.09	4.29
L =10 m												
Case 1.1	6.13	2.01	0.14	1.14	6.45	1.12	0.08	0.27	3.52	2.06	0.07	0.16
Case 1.2	9.38	6.15	0.63	2.66	5.84	1.18	0.05	0.27	1.79	0.77	0.01	0.23
Case 1.3	10.40	6.09	0.89	1.40	4.29	0.77	0.02	0.29	4.98	1.86	0.02	0.34
Case 1.4	11.79	9.28	2.90	6.47	5.67	1.06	0.00	0.42	2.19	0.98	0.04	0.31
Case 1.5	8.30	7.85	4.74	4.99	7.24	5.44	0.48	1.10	6.32	5.42	0.26	0.57
Case 2.1	8.74	7.55	0.39	7.67	14.39	2.26	6.04	4.20	13.02	4.57	3.98	3.88
Case 2.2	8.04	3.03	7.17	9.54	8.22	8.80	2.44	4.38	5.63	2.71	3.65	3.82
Case 2.3	2.25	7.87	6.23	1.90	2.73	5.63	0.18	4.55	1.60	4.61	7.63	3.94
Case 3.1	7.86	5.90	6.45	7.21	15.28	3.22	7.65	4.57	14.26	4.22	1.70	4.16
Case 3.2	7.18	1.79	4.11	9.25	9.07	9.81	3.85	4.90	6.28	3.30	4.72	4.55
Case 3.3	3.43	7.55	5.37	2.87	3.59	6.61	10.36	5.14	1.17	5.18	8.35	4.71

Table 5 shows the calculation error of each working condition. The error range is the same as in the references [17]. In the high-pressure situation (45 bar), for homogeneous isothermal conditions, the maximum error of wall heat flux is 10.80 % (case 1.5,1 m). The max error of average heat flux is 5.42 % (case 1.5, 10 m), the max value of the midpoint source term error is 0.33 % (case 1.5, 5 m), and the max value of the average radiation source term error is 1.16 % (case 1.5, 1 m). For non-isothermal homogeneous conditions, the max error of wall heat flux is 13.02 % (case 2.1, 10 m). Besides, the max error of average heat flux is 6.53 % (case 2.1, 1 m), the max error of midpoint source term is 8.96 % (case 2.3, 5 m), and the max average radiation source term error is 4.11 % (case 2.3, 5 m). For non-isothermal and non-homogeneous conditions, the max error of wall heat flux is 14.26 % (case 3.1, 10 m). The max error of average heat flux is 8.42 % (case 3.1, 1 m), the max error of the midpoint source term is 8.35 % (case 3.3, 10 m), and the max average radiation source term error is 4.71 % (case 3.3, 10 m). Meanwhile, as the pressure decreases, the average error decreases at 1 bar and 5 bar. Overall, the error increases with temperature. For non-isothermal conditions, the error values are higher than those for isothermal conditions. This is because the existence and change of temperature difference will complicate the heat transfer process, especially the effect on heat flux. The error is also relatively small under non-homogeneous, indicating that the model is suitable for practical engineering calculations.

3.5.2 The effect of pressure on the average heat flux

This study also explored the impact of pressure on the average heat flux in one dimension (S = 1 m). We compare the average heat flux for three conditions at pressures of 1, 5, and 45 bar with a temperature change of 1000 – 2000 K.

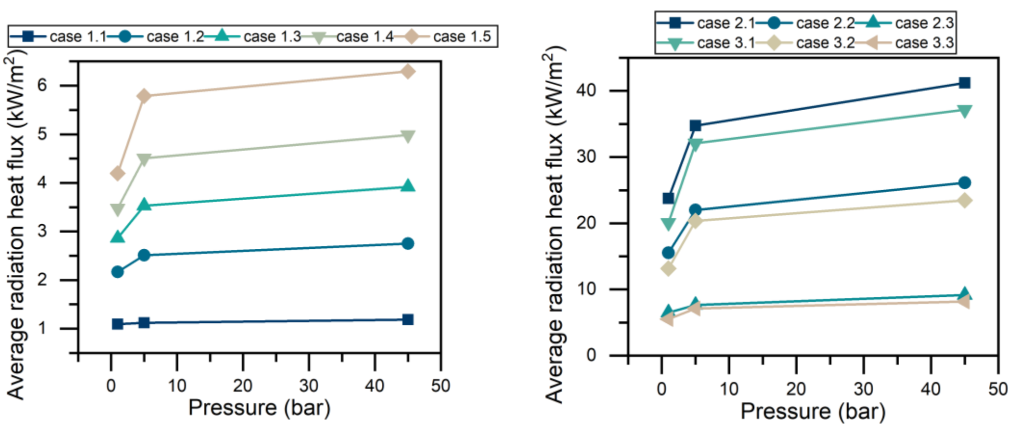

(a) isothermal cases (b) non-isothermal cases

Fig. 19 The effect of pressure on the average radiation heat flux

Figure 19 shows the effect of pressure on radiation heat flux for (a) isothermal and (b) non-isothermal conditions. The average radiation heat flux saw a gradual increase with pressure on each figure. Meanwhile, the radiation heat flux in Figure 19 (a) shows a law that increases with temperature. As indicated in Figure 19 (b), the larger the magnitude of the temperature change, the higher the average heat flux. It can also be seen from Figure 19 (a) that when the pressure increases from 1 bar to 5 bar, the higher the temperature, the more significant the increase in the average heat flux. It shows that the pressure at high temperatures significantly influences the radiation heat transfer of the mixed flue gas. In addition, the higher the temperature, the higher the average radiative heat flux. Therefore, the radiation heat transfer intensity of the mixed flue gas in the high gasification temperature and high-pressure equipment is very high. In Figure 19 (b), under the same pressure change, the larger the temperature change range, the more extensive the average heat flow increase range. In addition, Figure 19 (b) also shows that change affects the average heat flux in the case of non-homogeneous gas components. In engineering applications, we need to consider the gas component changes accompanying the reaction to simulate heat transfer calculation in solar gasification.

4 Conclusion

The comprehensive utilization of carbon-containing raw materials in a low-carbon and resourceful manner is one of the development directions of the global energy strategy. This investigation successfully developed a new WSGG model for solar gasification (using CO_2 as the gasification agent). The new WSGG model is applied to one-dimensional radiation heat transfer cases. At the same time, we verify the new model's accuracy, which agrees well with the benchmark model. Furthermore, we extend the applicable pressure range of the new WSGG model, which will be applied in the engineering of solar gasification. To sum up, we reach the following conclusions:

(1) A new WSGG model was developed based on CO and CO_2 mixed gas for solar-driven carbon-containing feedstock gasification. The emissivity database of the new WSGG model matches the benchmark (SNB) model database well. The total emissivity of the mixed gas increases with pressure but decreases with temperature.

(2)For the first time, this study explored the case where the H/C element ratio is 0. Compared with previous WSGG models, the new WSGG model has a good emissivity match with the benchmark (SNB) model under this condition. So, it is necessary to develop a new model for the gaseous radiation medium with a H/C element ratio of 0.

(3)Based on the DOM, this study solved 1-D RTE for three typical conditions (isothermal homogeneity, non-isothermal homogeneity and non-isothermal non-homogeneity) under three different typical pressures (1 bar, 5 bar, 45 bar). The results show that the difference in the average radiation source term between the new WSGG model and the benchmark SNB model is within 5% in common solar gasification engineering condition (5 bar, 5 m).

(4)This study discusses the effects of pressure, temperature, and path lengths on the radiation heat transfer of gases. The results show that the average heat flux increases with the pressure. Meanwhile, the higher the temperature, the more significant the increase in the average heat flux. It shows that pressure substantially influences the radiation heat transfer of the mixed flue gas under high-temperature conditions. Furthermore, the greater the magnitude of the temperature change, the higher the average heat flux. In the practical application of solar gasification, different reaction zone temperatures have various composition changes. The above results show that the new WSGG model will provide an accurate model for applying solar gasification engineering.

Acknowledgments

The work is financially supported by the Science and Technology Department of Ningxia Province (No. 2018BCE01004), the National Natural Science Foundation of China (52206175), China Postdoctoral Science Foundation (2021M702793), the China Scholarship Council (202106320152), Zhejiang University Ph.D. Academic Rising Star Program (2022035), and Qingshan Overseas Exchange Scholarship.

Support from the UK Engineering and Physical Sciences Research Council under the project “UK Consortium on Mesoscale Engineering Sciences (UKCOMES)” (Grant No. EP/X035875/1) is gratefully acknowledged.

Appendix

Table A1 New WSGG model parameters in 1 bar.

MR		0.125---0.5			0.5---1			1---4	
	A2	B2	C2	A2	B2	C2	A2	B2	C2
K1	0.191533632	-0.09887916	0.017742553	0.133625936	-0.156430496	0.060995145	-0.005883235	0.024156016	0.019917804
K2	1.706964949	-1.052964648	0.274810374	1.4479866	-1.742344262	0.684244768	-0.090822864	0.414917239	0.065792731
K3	7.039469728	-3.670780956	1.611154154	11.1190717	-13.25693867	5.384332519	-0.213471334	1.006442604	2.45349428
K4	-9.65058272	21.67609476	19.04698096	232.9659102	-283.6041406	111.0329754	4.96298454	-17.15626561	72.58802609
	A1	B1	C1	A1	B1	C1	A1	B1	C1
c14	-32.13355834	22.49946505	-2.486164426	-2.227066824	3.52774739	-0.476928475	0.060673677	-0.130585887	0.893664301
c13	100.9945686	-71.130903	7.968161704	7.852628008	-12.21044188	1.793416292	-0.215000197	0.476692699	-2.826090084
c12	-109.5929312	77.78202144	-8.878508838	-9.662666232	14.75455507	-2.347341896	0.26686999	-0.597371847	3.0750488
c11	48.58502075	-34.5390938	3.853166474	4.646273072	-6.960298412	1.048455701	-0.128649374	0.275852149	-1.412772414
c10	-9.507255488	6.361424128	-0.435219497	-0.69522904	0.99321692	0.045877495	0.016865609	-0.025145011	0.352144777
c24	5.477980395	-4.829294936	0.847384035	-0.752989904	0.599139344	-0.30909053	0.04398543	-0.285888007	-0.221038513
c23	-16.36710908	14.74758402	-2.476143172	2.448001344	-1.973922304	1.180832383	-0.129611401	0.855253773	0.929269051
c22	16.1681455	-15.0122801	2.308840129	-2.905762248	2.485205378	-1.671425672	0.129308672	-0.866765554	-1.354525661
c21	-5.134741696	5.135126624	-0.672387685	1.659299128	-1.670855874	1.032093358	-0.051270351	0.330256427	0.741550536
c20	0.015097621	-0.207454936	0.084095794	-0.378051304	0.453258318	-0.147973602	0.009325749	-0.042991285	-0.039101052
c34	-3.461617269	2.547742548	-0.356278968	0.584851184	-0.685612984	0.248781685	-0.049809352	0.250445231	-0.052615993
c33	9.632228864	-7.251337048	1.191132418	-2.25624556	2.707762822	-0.816298911	0.166420706	-0.832738478	0.301536123
c32	-8.053838315	6.299859888	-1.374224925	3.062567712	-3.736440252	0.864823638	-0.194157755	0.968109899	-0.583001046
c31	1.561462069	-1.37985002	0.557284071	-1.800516016	2.240267764	-0.4122803	0.085773227	-0.423911991	0.365610212
c30	-0.154195179	0.140744784	-0.005734449	0.326490024	-0.418344934	0.153639109	-0.005879101	0.029512212	0.038151089
c44	-0.168970229	0.56256962	-0.714184259	0.014130016	0.158732748	-0.558040884	-0.003316101	0.074513975	-0.456375995
c43	0.462189493	-1.710000676	2.407395812	-0.178659888	-0.367635584	1.896425611	0.008914564	-0.22487815	1.566093725
c42	-0.553926784	1.90038024	-2.838336538	0.437421032	0.127583586	-2.199775165	-0.009139274	0.23582066	-1.861451933
c41	0.53605024	-1.062415432	1.282685165	-0.180409568	-0.080766064	0.970975433	0.005269176	-0.104621525	0.809152151
c40	-0.347438475	0.372842388	-0.118010656	-0.179050416	0.279529912	-0.113451433	-0.002046163	0.022578556	-0.03350433

Table A2 New WSGG model parameters in 5 bar.

MR		0.125---0.5			0.5---1			1---4	
	A2	B2	C2	A2	B2	C2	A2	B2	C2
K1	-0.050028565	0.036850464	0.042958584	-0.058315096	0.064873618	0.03101864	-0.004753783	0.02963038	0.012700565
K2	-3.629284853	2.54624158	0.123288917	0.31383772	-0.878479342	0.849868735	-0.076846512	0.44820242	-0.086128795
K3	-45.19035566	38.03486002	-0.7697375	23.946928	-43.9017233	22.91423325	-1.618342482	8.545129354	-3.967348929
K4	212.4322517	-0.9497004	83.02453787	1057.781621	-1687.208667	714.8166789	-41.47234459	208.7885197	-81.92654225
	A1	B1	C1	A1	B1	C1	A1	B1	C1
c14	-12.12366624	9.843743984	0.229170637	-2.21559644	2.879741786	1.234154286	-0.051309198	0.249547011	1.700061819
c13	39.27226658	-32.02467922	-0.687984428	7.226020312	-9.411911082	-3.982806928	0.172553249	-0.831140048	-5.5101109
c12	-44.36678644	36.30171488	0.693986893	-8.042667664	10.46405356	4.531787858	-0.195532255	0.926282949	6.222423065
c11	19.9867115	-16.24613258	-0.395110109	3.378056112	-4.235349372	-2.248337866	0.089035467	-0.411800911	-2.782865682
c10	-3.034022261	2.34325222	0.234978169	-0.37598876	0.337036042	0.573577883	-0.018848432	0.089687657	0.46378594
c24	4.34140704	-2.515344936	-0.135298488	1.251243864	-0.633827738	-0.303516293	0.059118014	-0.247263664	0.502045483
c23	-13.627721	7.836775184	0.576210365	-4.286198032	2.243121328	1.03765655	-0.2239386	0.971682987	-1.753164541
c22	15.3762392	-8.703116996	-0.870079405	4.836162504	-2.268603338	-1.45231706	0.288911383	-1.27912572	2.105456443
c21	-6.772706773	3.53207068	0.552184294	-1.862807104	0.3351342	0.923177617	-0.142013357	0.627442834	-1.089924764
c20	0.567945845	-0.073044444	-0.069015615	0.216260504	0.085961526	-0.060597265	0.019258903	-0.083434397	0.305800259
c34	-2.38062288	0.289096484	0.751343699	0.434115248	-1.381998004	0.883206411	0.043785894	-0.376979134	0.268516894
c33	6.928459829	-0.35110742	-2.252193034	-0.562746256	3.136791492	-2.123340969	-0.123160528	1.117250955	-0.54338616
c32	-7.055726091	-0.20230558	2.181025828	-0.377308728	-1.845237074	1.332887234	0.12961083	-1.189700101	0.170430703
c31	2.554930229	0.52660166	-0.765379926	0.336921872	0.4202846	-0.157719307	-0.064379601	0.543299468	0.120567298
c30	0.022296256	-0.293420112	0.166808964	0.237232168	-0.45592663	0.194328245	0.007882829	-0.068732389	0.036483343
c44	2.317473483	-0.53312866	-1.11135086	-0.09628588	0.622371546	-1.085661122	-0.030256301	0.257838833	-0.787157988
c43	-6.786512075	1.154790084	3.808151052	-0.34295028	-0.828311582	3.188811436	0.114128557	-0.932380234	2.835801251
c42	6.309794731	-0.28805984	-4.566611434	1.329296856	-0.838151478	-3.046441146	-0.16561046	1.253768768	-3.643454076
c41	-1.761672288	-0.631454332	2.084232435	-0.896122352	1.037458896	1.033388337	0.098496709	-0.686241962	1.762470133
c40	0.028329013	0.230253532	-0.170189363	-0.16597056	0.331768204	-0.172371806	-0.005942174	0.055457019	-0.056089007

Table A3 New WSGG model parameters in 45 bar.

MR		0.125---0.5			0.5---1			1---4	
	A2	B2	C2	A2	B2	C2	A2	B2	C2
K1	-0.781214592	0.572707104	-0.001804331	-0.41835516	0.511105602	-0.061718438	-0.02843442	0.179817622	-0.120351197
K2	-7.995585579	5.564168032	-0.168422665	-1.49720964	1.899421854	0.039356439	-0.223469993	1.393471833	-0.728433187
K3	-36.24985805	27.81160354	0.184280212	-10.92226943	13.95793102	0.779219321	-2.066913371	14.78970044	-8.907906158
K4	585.3155285	-77.6649112	112.7660915	-127.122684	182.4491674	160.8186053	-48.24330073	295.5591948	-31.17080537
	A1	B1	C1	A1	B1	C1	A1	B1	C1
c14	-4.641626571	0.8679341	1.122126506	-0.913486792	0.530716222	0.3587005	-0.089204716	0.527293748	-0.462159102
c13	13.8950117	-2.037608676	-3.651860625	3.045987752	-1.83015961	-1.043329171	0.322795431	-1.915717713	1.765421253
c12	-14.56343491	1.558123836	4.113140492	-3.571032712	2.23285973	1.027671995	-0.40194176	2.387227302	-2.295786528
c11	6.277448779	-0.519730996	-1.839981311	1.63165888	-1.0393996	-0.418699534	0.19107953	-1.125505556	1.107985772
c10	-1.171955797	0.204122072	0.321454123	-0.257580584	0.157958534	0.115942089	-0.032240132	0.187756815	-0.139196644
c24	-4.691688949	4.764845156	0.784828852	-1.492865944	1.81168681	1.461702274	-0.177080788	1.023650295	0.933953633
c23	15.58928976	-15.76268764	-2.581156894	5.106362248	-6.202374494	-4.740581591	0.580136683	-3.329341142	-3.087389378
c22	-17.68227983	17.83283022	3.019924619	-5.926654408	7.148457098	5.423204823	-0.662139958	3.763788249	3.543359222
c21	7.796103061	-7.674493752	-1.575626468	2.623688144	-3.017776536	-2.610881347	0.312561222	-1.760658197	-1.556872764
c20	-1.198923595	1.04130514	0.392233348	-0.318867104	0.301968036	0.541887777	-0.057115246	0.324067592	0.258036363
c34	6.689322453	-3.92903692	0.089617946	2.452006328	-1.619848546	-0.00564721	0.37354576	-2.276651967	2.729616779
c33	-23.86183293	14.20989144	-0.277126721	-8.656641288	6.180566974	-0.0637624	-1.247706998	7.586852665	-8.878982381
c32	29.32706742	-17.58585561	0.171329663	10.4953673	-7.869080622	0.020867198	1.464715128	-8.865041226	10.04747998
c31	-14.40914736	8.451886428	0.056443155	-4.838423688	3.559802406	0.109804248	-0.699933223	4.196398376	-4.665282187
c30	2.678287947	-1.445364756	0.08197329	0.654568976	-0.397478364	0.063959837	0.112856801	-0.667925219	0.876118867
c44	2.105784587	-1.608366228	-0.32639108	-0.340637376	-0.45138428	-0.293276563	-0.126830998	0.831815426	-1.790282647
c43	-4.286421707	3.4695617	1.641315574	1.641784016	0.688134784	1.549977601	0.426052312	-2.804574128	6.258418216
c42	1.61907952	-1.638867524	-2.712809766	-2.519616432	0.195225468	-2.595182274	-0.515443212	3.3947943	-7.798924326
c41	0.946478496	-0.466783396	1.580581019	1.329766024	-0.409721206	1.456228042	0.25597678	-1.675960014	3.796256094
c40	-0.367505557	0.235937416	-0.064556011	-0.098364736	-0.028260176	0.00025758	-0.028036587	0.183971008	-0.282301753

References

[1] Freda C, Tarquini P, Sharma VK, Braccio G. Thermodynamic improvement of solar driven gasification compared to conventional one. Energy 2022;261.

[2] Wang X, Liu Y, Bi J, Liu M. New challenges of the Belt and Road Initiative under China's "3060" carbon target. Journal of Cleaner Production 2022;376.

[3] Li X, Chen J, Lipiński W, Dai Y, Wang C-H. A 28 kWe multi-source high-flux solar simulator: Design, characterization, and modeling. Solar Energy 2020;211:569-83.

[4] Fang Y, Paul MC, Varjani S, Li X, Park Y-K, You S. Concentrated solar thermochemical gasification of biomass: Principles, applications, and development. Renewable and Sustainable Energy Reviews 2021;150.

[5] Zhang Q, Shan S, Yu J, Zhou Z, Luo KH. Coal gasification process driven by concentrated solar radiation for carbon neutralization: Reaction and energy characteristics. Chemical Engineering Journal 2022;450.

[6] Janajreh I, Adeyemi I, Raza SS, Ghenai C. A review of recent developments and future prospects in gasification systems and their modeling. Renewable and Sustainable Energy Reviews 2021;138.

[7] Rivière P, Soufiani A. Updated band model parameters for H2O, CO2, CH4 and CO radiation at high temperature. International Journal of Heat and Mass Transfer 2012;55(13-14):3349-58.

[8] Smith TF, Shen ZF, Friedman JN. Evaluation of Coefficients for the Weighted Sum of Gray Gases Model. J Heat Trans-T Asme 1982;104(4):602-8.

[9] Yin C, Johansen LCR, Rosendahl LA, Kær SK. New Weighted Sum of Gray Gases Model Applicable to Computational Fluid Dynamics (CFD) Modeling of Oxy−Fuel Combustion: Derivation, Validation, and Implementation. Energy & Fuels 2010;24(12):6275-82.

[10] Rehfeldt S, Kuhr C, Ehmann M, Bergins C. Modeling of radiative properties of an Oxyfuel atmosphere with a weighted sum of gray gases for variable carbon dioxide and water vapor concentrations. Energy Procedia 2011;4:980-7.

[11] Johansson R, Leckner B, Andersson K, Johnsson F. Account for variations in the H2O to CO2 molar ratio when modelling gaseous radiative heat transfer with the weighted-sum-of-grey-gases model. Combustion and Flame 2011;158(5):893-901.

[12] Kangwanpongpan T, França FHR, Corrêa da Silva R, Schneider PS, Krautz HJ. New correlations for the weighted-sum-of-gray-gases model in oxy-fuel conditions based on HITEMP 2010 database. International Journal of Heat and Mass Transfer 2012;55(25-26):7419-33.

[13] Dorigon LJ, Duciak G, Brittes R, Cassol F, Galarça M, França FHR. WSGG correlations based on HITEMP2010 for computation of thermal radiation in non-isothermal, non-homogeneous H_2O/CO_2 mixtures. International Journal of Heat and Mass Transfer 2013;64:863-73.

[14] Selhorst AHB, Fraga GC, Coelho FR, Bordbar H, França FHR. A Compact WSGG Formulation to Account for Inhomogeneity of H2O–CO2 Mixtures in Combustion Systems. Journal of Heat Transfer 2022;144(7).

[15] Wang B, Xuan Y. An improved WSGG model for exhaust gases of aero engines within broader ranges of temperature and pressure variations. International Journal of Heat and Mass Transfer 2019;136:1299-310.

[16] Wu X, Fan W, Liu S, Chen J, Guo H, Liu Z. A new WSGGM considering CO in oxy-fuel combustion: A theoretical calculation and numerical simulation application. Combustion and Flame 2021;227:443-55.

[17] Shan S, Zhou Z, Chen L, Wang Z, Cen K. New weighted-sum-of-gray-gases model for typical pressurized oxy-fuel conditions. International Journal of Energy Research 2017;41(15):2576-95.

[18] Shan S, Qian B, Zhou Z, Wang Z, Cen K. New pressurized WSGG model and the effect of pressure on the radiation heat transfer of H2O/CO2 gas mixtures. International Journal of Heat and Mass Transfer 2018;121:999-1010.

[19] Cai X, Shan S, Zhang Q, Zhao J, Zhou Z. New WSGG model for gas mixtures of H2O, CO2, and CO in typical coal gasifier conditions. Fuel 2022;311.

[20] Puig-Arnavat M, Bruno JC, Coronas A. Review and analysis of biomass gasification models. Renewable and Sustainable Energy Reviews 2010;14(9):2841-51.

[21] Islam S, Kopyscinski J, Liew SC, Hill JM. Impact of K2CO3 catalyst loading on the CO2-gasification of Genesse raw coal and low-ash product. Powder Technology 2016;290:141-7.

[22] Chu H, Gu M, Consalvi J-L, Liu F, Zhou H. Effects of total pressure on non-grey gas radiation transfer in oxy-fuel combustion using the LBL, SNB, SNBCK, WSGG, and FSCK methods. Journal of Quantitative Spectroscopy and Radiative Transfer 2016;172:24-35.

[23] Anouar Soufiani JT. High temperature gas radiative property parameters of statistical narrow-band model for H_2O, CO_2 and CO, and correlated-K model for H_2O and CO_2. International Journal of Heat and Mass Transfer 1997;40(4):987-91.

[24] Qin W, Wang L, Wei J, Hu B, Liang X. A novel efficient broadband model to derive daily surface solar Ultraviolet radiation (0.280-0.400 mum). Sci Total Environ 2020;735:139513.

[25] Malkmus W. Random Lorentz Band Model with Exponential-Tailed S−1 Line-Intensity Distribution Function. Journal of the Optical Society of America 1967;57(3):323-9.

[26] Zheng S, Sui R, Yang Y, Sun Y, Zhou H, Lu Q. An improved full-spectrum correlated-k-distribution model for non-gray radiative heat transfer in combustion gas mixtures. International Communications in Heat and Mass Transfer 2020;114.

[27] Li H, Zhang J, Cheng Y, Huang Z. Calculations of radiative intensity in one-dimensional gaseous media with black boundaries using the statistical narrow band model. Journal of Quantitative Spectroscopy and Radiative Transfer 2020;240.

[28] Zheng S, Yang Y, Zhou H. The effect of different HITRAN databases on the accuracy of the SNB and SNBCK calculations. International Journal of Heat and Mass Transfer 2019;129:1232-41.

[29] Hottel HC, Saforim AF. Radiative transfer. 1967.

[30] Hecht ES, Shaddix CR, Geier M, Molina A, Haynes BS. Effect of CO2 and steam gasification reactions on the oxy-combustion of pulverized coal char. Combustion and Flame

2012;159(11):3437-47.

[31] Piatkowski N, Wieckert C, Weimer AW, Steinfeld A. Solar-driven gasification of carbonaceous feedstock—a review. Energy Environ Sci 2011;4(1):73-82.

[32] Loutzenhiser PG, Muroyama AP. A review of the state-of-the-art in solar-driven gasification processes with carbonaceous materials. Solar Energy 2017;156:93-100.

[33] Abanades S, Rodat S, Boujjat H. Solar Thermochemical Green Fuels Production: A Review of Biomass Pyro-Gasification, Solar Reactor Concepts and Modelling Methods. Energies 2021;14(5).

Declaration of interests

The authors declare that they have no known competing financial interests or personal relationships that could have appeared to influence the work reported in this paper.